Advances in Geo-Energy Research

Vol. 6, No. 3, p. 221-229, 2022

Invited review

Nanoscale pore and crack evolution in shear thin layers of shales and the shale gas reservoir effect

Yan Sun[1], Yiwen Ju[2]*, Wei Zhou[1], Peng Qiao[2], Liru Tao[2], Lei Xiao[2]

[1]*State Key Laboratory for Mineral Deposit Research, School of Earth Sciences and Engineering, Nanjing University, Nanjing 210093, P. R. China*

[2]*Key Laboratory of Computational Geodynamics, College of Earth and Planetary Sciences, University of Chinese Academy of Sciences, Beijing 100049, P. R. China*

Keywords:
Shale
shear thin layers
pore and crack
shale gas
reservoir effect

Cited as:
Sun, Y., Ju, Y., Zhou, W., Qiao, P., Tao, L., Xiao, L. Nanoscale pore and crack evolution in shear thin layers of shales and the shale gas reservoir effect. Advances in Geo-Energy Research, 2022, 6(3): 221-229.
https://doi.org/10.46690/ager.2022.03.05

Abstract:
Studies on matrix-related pores from the nanometer to the micrometer scale in shales have made considerable progress in recent decades. However, nanoscale pores and cracks developed in the shear thin layers have not been systematically discussed. In this work, interlayer shear slip occurring in shales are observed through practical examples. The results show that the shear thin layer constructed by nanograin coating is widely distributed on superimposed shear slip planes. Usually, the development of the shear thin layer undergoes viscoelastic-rheological-embrittling deformation stages, and the nanograin texture assembled in the shear thin layer can demonstrate three pore and crack structure types. Based on the mechanical analysis concerning nanoscale cohesion force, it is identified that, as long as force remains a state, the shear thin layer must bear a nanoscale pore and crack character. Furthermore, the shale gas reservoir effect of the nanoscale pore and crack is simply discussed. Obviously, the adsorbed gas effect of the nanograin itself has a larger nanoscale size and surface functionality than those of kerogen and clay particles in the shales; three structure types of the nanoscale pore and crack can act as given controlling factors of storage and permeability for the free gas. Both the matrix-related pores and the three pore and crack structures have an intimate connection with respect to each other in the genetic mechanism and temporal-spatial evolution. This work has important theoretical implications for supplementing the pore and crack classification of shale. Moreover, it makes a significant contribution to shale gas exploration and development.

1. Introduction

Unconventional natural gas has raised increasing research interest for potential oil-gas exploration on a global scale (John and Roger, 2007; Comer, 2008). Shale gas reservoirs are unusual forms of hydrocarbon accumulation, and matrix porosity and well-developed cracks are important factors for scale gas enrichment. Undeniably, pores and cracks can provide not only shale gas accumulation space, but also allow for migration pathways of gas production (Montgomery et al., 2005; Long et al., 2011; Ju et al., 2016, 2017).

Pore and crack in the shales (including shale and mudstone (Javadpour, 2009; Loucks et al., 2012)) of unconventional natural gas reservoirs, including their physical characterization, forming condition and deformation mechanism, have been studied both at the macro- and microscale by various methods since the 1970s (Curtis, 2002; Gale et al., 2007; Chen et al., 2009; Wang and Ju, 2015; Zhu et al., 2019); however, studies on those phenomena at the ultra-microscopic scale and nano level were seldom performed. Nowadays, researches about nano minerals, nano geochemistry and nano petrofabrics have progressively increased geologists' attention (Hochella et al., 2008; Wang et al., 2011; Ju et al., 2017, 2018), thus nanosized pores and nanoscale cracks (including nanogrooves (Javadpour, 2009)) have been extensively observed in different rocks and borehole depths (Desbois et al., 2009; Loucks et al., 2009; Janssen et al., 2011; Li et al., 2020). Moreover, a

Yandy Scientific Press

*Corresponding author.
E-mail address: sunyan37@sina.com (Y. Sun); juyw03@163.com (Y. Ju); wei.zhou8906@gmail.com (W. Zhou); qiaop1996@163.com (P. Qiao); taoliru2018@163.com (L. Tao); xiaolei191@mails.ucas.ac.cn (L. Xiao).

Received March 15, 2022; revised April 10, 2022; accepted April 16, 2022; available online April 18, 2022.

strong nanometer effect has been recognized in clay minerals, deformed coal and shales (Aringhieri, 2004; Slatt and O'Brien, 2011; Ju et al., 2017). Obviously, the new paradigms continue to offer numerous and substantial challenges that naturally accompany the developing process of nanoscale pores and cracks in unconventional shale reservoirs. There is general consensus that the understanding and recognition of a developed stage and the generative mechanism of pore and crack in the shales at the nanoscale are vital for the theoretical analysis and practical exploration of shale reservoirs.

It should be emphasized that shale matrix-related pores composed of nanometer- to micrometer-size pores have been well documented and discussed for a shale gas system, such as regarding pore type, classification and genetics (Desbois et al., 2009; Javadpour, 2009; Loucks et al., 2009; Slatt and O'Brien, 2011; Chen et al., 2017). However, unlike the matrix-related pore, the nano (or micro-nano) level pore and crack developed in the shear thin layers have not been systematically analyzed. Therefore, the pore and crack evolution in shale tectonic shear zone and its relationship with shale gas occurrence need further investigation.

In this work, layer-slipping and shear thin layers are observed through practical examples. Strain phenomena and the frictional effect produced on the interlayer are found to be widespread in soft bed deformation. Then, the developing process and the order of pore and crack are divided into different stages. Finally, the shale reservoir behavior and nano-effects are synthetically considered and analyzed. The findings are of great relevance to the development of tectonic geology theory and make a significant contribution to shale gas exploration and development.

2. Layer-slipping and shear thin layers

2.1 Layer-slipping

Layer-slipping, which gives rise to various interlayer motions and structures, is extensively found at different levels and in different rocks, especially in the shale bedding (Suvorov, 2000; Morley et al., 2017). As a pool of data of the "digital stratum" (Tahirkheli, 2001) for analysis, the mechano-physical properties of samples collected from the Changqing oil-gas field were shown in Table 1. The differences in the mechano-physical parameters between soft shale bed (C_{2b}) and hard country rock bed (O_{1m}) are conspicuous, and the layer slipping tends to occur in the argillutite with higher Poisson's ratio and smaller Young's modulus than in the neighboring rocks.

2.2 Shear thin layers

Shear thin layers that can lead to a series of new nano-mineral materials, new nanofabricated textures (Krása et al., 2014), nanometer schistose-grain texture, and nanometer layer-grain texture (Sun et al., 2008c), are the focus of research on the slipping micro-mechanism of the fault zone (De Paola, 2013), and these phenomena commonly occur on the shearing planes, both on a brittle shear surface and a ductile shear one. Nano mineral materials on the former indicate a thick coating shell called shear thin layer or dynamic thin shell (Sun et al., 2008b), with an mm-cm grade of single thickness, and the latter is commonly a very thin layer with μm-cm grade of single thickness (Fig. 1, Table 2).

At the mesoscopic scale, there are no traces of slickenside and schlieren on the surfaces of shear slipping, and they only exhibit a light silk luster. Under scanning electron microscopy (SEM), in the shear thin layers, a layered texture, pore and crack can be found on the shearing surfaces (Fig. 1). Likewise, they can be seen in the sample compression experiment (Table 2, Fig. 2).

3. Three developing stages of nanoscale pore and crack

Based on the observation and study of nano-coating textures (Sun et al., 2008a, 2013), three evolutionary stages of the nanoscale pore and crack system in the shales have been

Table 1. Physical parameters of shale and dolomite (Sun et al., 2003).

Rock bed	Sample collection	Poisson's ratio	Modulus (10^{10} Pa)			Lame constant	Wave velocity (m/s)	
			Young's	Shear	Volume	(10^{10} Pa)	Longitudinal	Latitudinal
Cabargillite (C_{2b})	Parallel to bed	0.330	4.52	1.79	3.14	1.95	5404	2845
	Perpendicular to bed	0.363	4.93	1.81	6.00	4.79		
Powdery crystalline dolomite (O_{1m})	Parallel to bed	0.245	5.82	2.34	3.80	2.24	5442	2798
	Perpendicular to bed	0.310	5.92	2.28	5.19	3.68		

Table 2. Experimental parameters of triaxial pressure of shale (dry condition).

No.	Size (mm)	Experimental parameters					
		Axial pressure (MPa)	Confining pressure (MPa)	Temperature (°C)	Duration (min)	Specimen shortening (mm)	Strain rate (10^{-6} s)
1 (Fig. 2(a))	51×19×19	166	50	400	410	7.3	5.82
2 (Fig. 2(b))	51×19×19	166	50	440	470	7.8	6.07

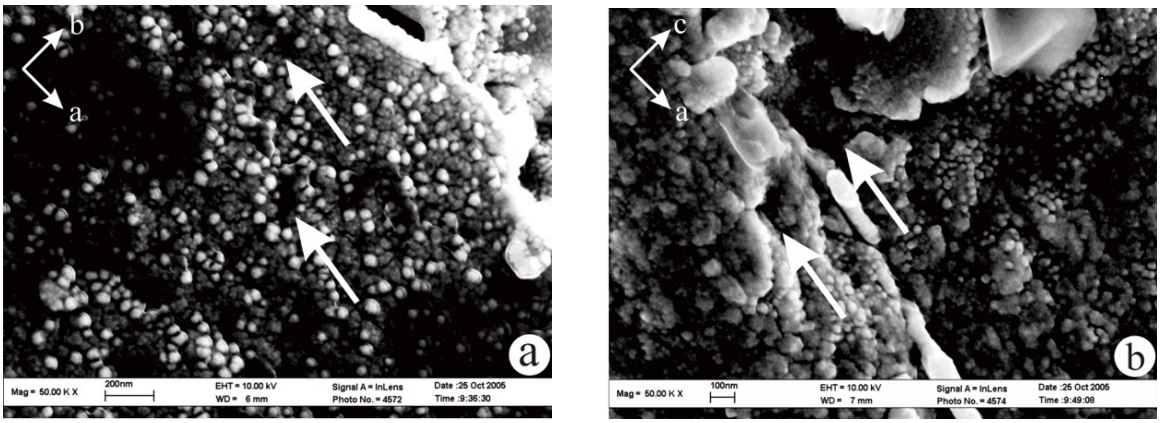

Fig. 1. SEM images of the surface of the shear thin layer of Permian shale from the South Yellow Sea basin: (a) Dense nanosized grains (with a diameter ranging from 25 to 45 nm) distributing on slip lamellae, where the arrows show nanoscale pores; (b) Superimposed layer texture (single bed with 50-80 nm thickness), where the arrows show nanograin arrangement and nanoscale cracks parallel to the axis a (Sun et al., 2018).

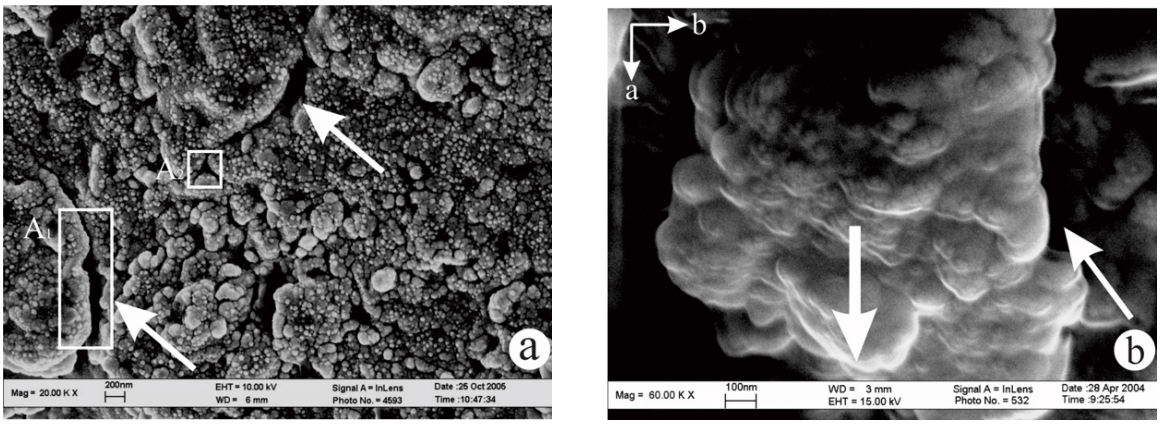

Fig. 2. SEM images of the surface of a shear thin layer from the HT/HP experiment: (a) Homogeneous distribution of nanograins (diameter, 45-55 nm) and its assembled bodies on a slip foliated plane, with the arrows indicating micro-nano scaled pore and crack between the assemblages (Sun et al., 2014b); (b) Compound nanograins and assemblages with pancake shapes, with the wide arrow indicating the front edge of plastic flow with a tongue shape feature, and deep cracks found on both of its sides.

suggested: viscous-elastic deformation according to synthetic analyses (Hunt and Peletier, 2000), ductile-brittle transformation (Mclaren and Pryet, 2001) and particle-slip rheology (Lu et al., 2005); these three stages are simply explained below.

3.1 Viscoelastic deformation stage

The contraction structure is formed by cohesion force during the viscoelastic deformation stage (Figs. 2(a) and 3(a)). Under shear strengthening, frictional-viscous slip (Urbakh et al., 2004), and viscous-elastic deformation, some individual nanograins with moderate roundness and sphericity can form on the lamellar surface through static grinding and kinetic friction (Braun and Naumovets, 2006) (Fig. 1). By virtue of the high strain rate, these granular nanograins (Fig. 1(a)) may concentrate into aggregated texture (Fig. 1(b)) and multi-aggregated texture (Fig. 2(a)). In light of the theoretical analysis, this phenomenon is caused by an internal cohesion force (Sun et al., 2014a). Meanwhile, only this force, which is also named contraction force to a piece formation of the nano aggregate grain, gives rise to the contraction deformation in the interlayer slipping shown in Fig. 2(a).

3.2 Rheological deformation stage

A relaxation structure is caused by unloading force during the rheological deformation stage (Figs. 2(b), 3(b) and 4). Under continual shear intensification strain softening (Holdsworth, 2004), temperature rise energy dissipation and grain-boundary sliding (Rainbourg et al., 2008) could all cause the self-weakening of dynamic evolution (Kealen et al., 2007), such that individual and aggregate nanograins will occur in rheological deformation, alienation and ductile flow phenomena (Goodwin and Wenk, 1995) (Fig. 4).

Grain boundary sliding and alienation extension occur along conjugate sliding lines (Fig. 4(a)), which are also called Luder's lines (Sun et al., 2008c), and this phenomenon manifests the typical characterization of plastic rheology (Fig.

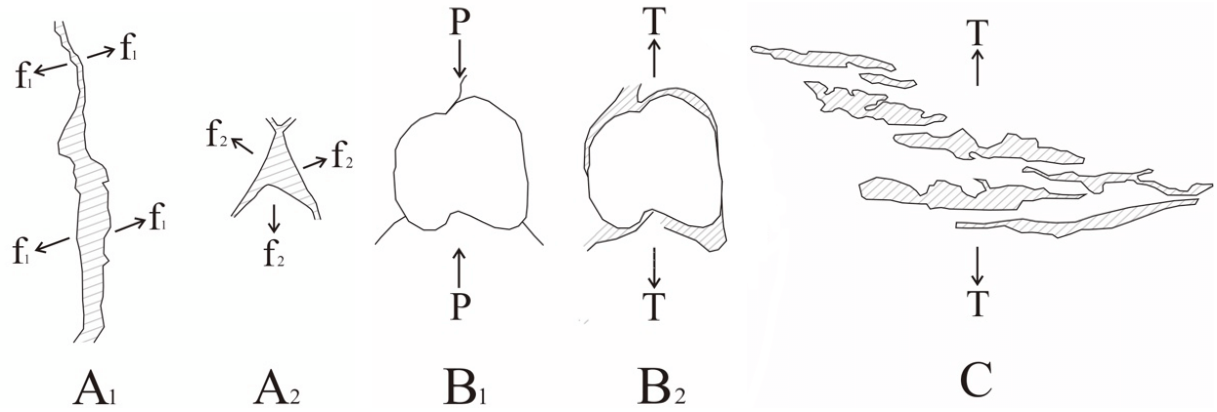

Fig. 3. A sketch of mechanical analysis for the nanoscaled pore and crack: (a) Contraction pore and contraction crack structure collected from microdomain A_1 and A_2 in Fig. 2(a), where f represents cohesible contraction force; (b) Relaxation structure collected from microdomain B in Fig. 4(b), where P shows compression force and T indicates tensile relaxation force; (c) Craze structure collected from microdomain C in Fig. 6(a), where T represents local tensile force.

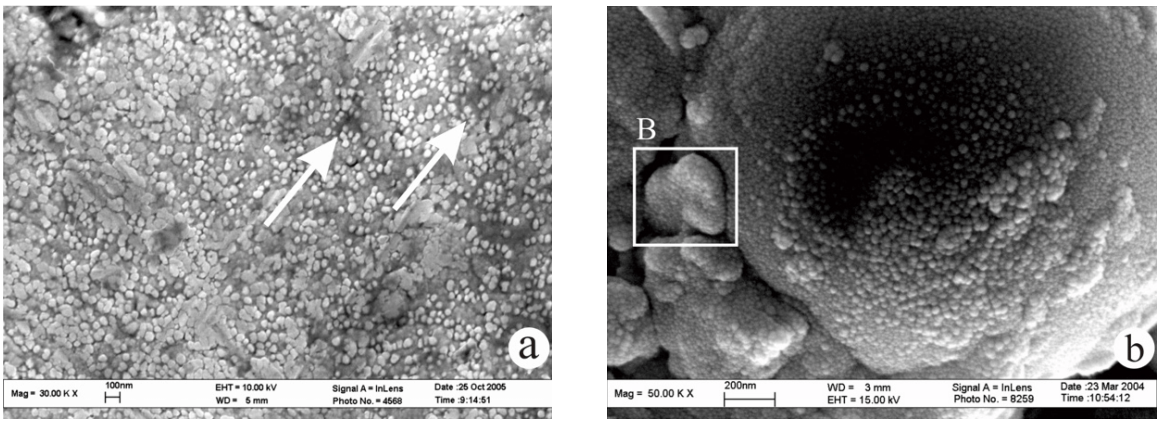

Fig. 4. SEM images of various nanoscaled structures in rheological deformation stages: (a) The original nanograins (diameter, 50-70 nm) were extended (length >100-150 nm) along the sliding line, and the micro-nanoscaled pore and crack are near the sliding line (Sun et al., 2008c); (b) Aggregate and multi-aggregate nanograins that were closely interdependent had been relieved, presenting a large rupture called crescent-shaped pore (Sun et al., 2008b).

2(b)). Commonly, a few nanoscaled pores and cracks distribute along or near the sliding lines (Fig. 4(a)). In this developing stage, relaxation is a significant structure (Fig. 4(b)), which is also called unloading fissure (Wang and Sun, 1990), and its production results from relief pressure force (Fig. 3(b)). The relaxation structure of pore and crack that has undergone compression-contraction might be incorporated into the contraction.

3.3 Embrittling deformation stage

The exfoliation structure is caused by spalling tension force during the embrittling deformation stage (Fig. 5(a)) (Hirose et al., 2006). Up to the third stage, this tectonic regime of deforming mechanism could perform an essential transition, i.e., from ductile shearing to brittle tensioning, because the intensive change had been strain decay (Kambe, 2001), with a few oxidation actions at the microscopic and mesoscopic scale. Therefore, in the embrittling deformation background, spalling tension force against the nanometer schistose-grain texture can lead to various pore and crack structures, especially exfoliation structures that are often found along the nanometer schistose-grain plane parallel to the ac fabric section (Fig. 5(a)).

3.4 Two further structures

The three developing stages mentioned above are closely relative and reiterative under many tectonization, tectonic metamorphism, and layer slipping actions. However, there are two other structures found in the shales, namely the delamination structure and the craze structure.

3.4.1 Delamination structure

The delamination structure caused by delaminating force easily appears along the nanometer layer-grain plane parallel to the shear slip (Guo et al., 2002). As such, in light of the ultra-microscopic analysis, the delaminated effect starts firstly, causing the separation of the nano-confinement layer (Berger,

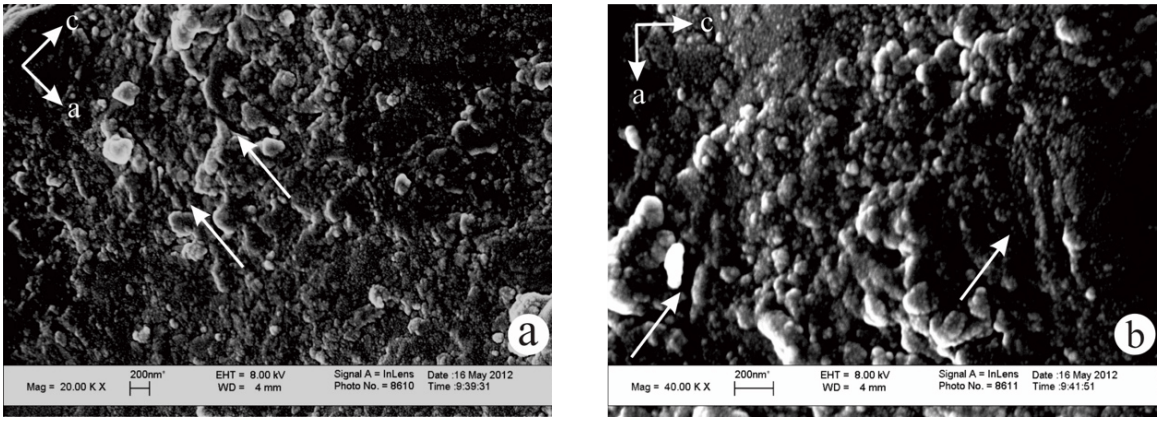

Fig. 5. SEM images of exfoliation and delamination structure: (a) Aggregate and multi-aggregate nanograins displaying a scaly texture, and exfoliation nanocracks with irregular appearances scattered along the fabric direction (Sun et al., 2017); (b) Delamination cracks appearing along the nanograin layers, which are reiterative with the exfoliation structure in the extension direction.

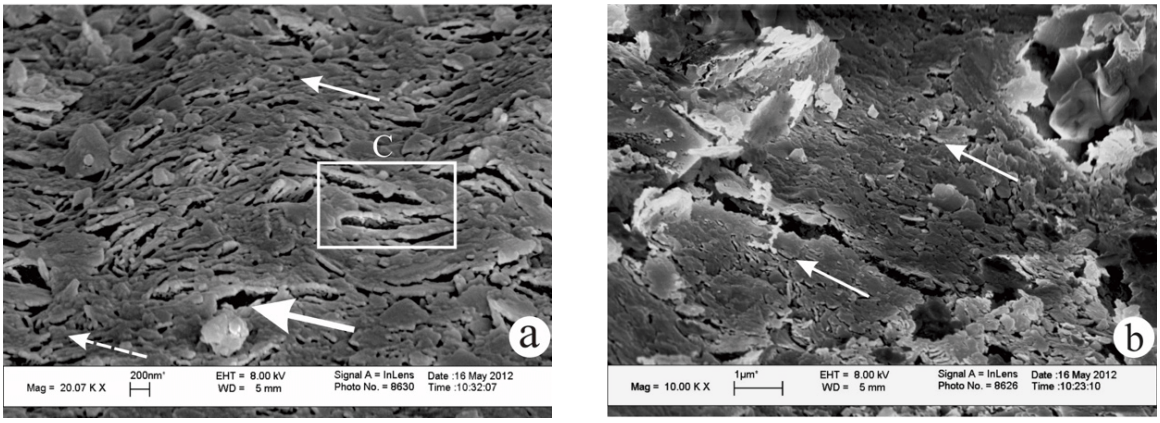

Fig. 6. SEM images of craze structure: (a) Craze pores and cracks with irregular shapes crowd together, forming clusters on the shear surface (Sun et al., 2014b), in which the grain boundaries display a blurred state (dotted line arrow); (b) Micrograde craze cracks parallel to nanoscaled craze, where the arrangement tendency of nanopores corresponds with the extension direction of the cracks.

1990), and the delamination structure that might occur at the first stage proposed above could manifest as a superimposed structure with the exfoliation crack through a compounding action at the third stage (Figs. 1(b) and 5(b)). Sometimes, the pore and crack presenting echelon arrays may be found under SEM. The schistose plane of exfoliation structure parallel to the delamination plane might be also merged into the delamination structure.

3.4.2 Craze structure

The craze structure is a peculiar damage phenomenon in glassy materials and neat glassy polymers (Berger, 1990), and its texture scale is mainly confined to micro and nano grade measurement (Luo and Yang, 1990). Notably, glassy pseudotachylite, which could result from frictional melting on the shear surface, has been investigated on a macroscopic/microscopic scale in more detail (Masch et al., 1995; Lin, 2008). In Fig. 6, a glassy material is shown at the ultra-microscopic scale. As compared with the normal case, this phenomenon demonstrates a melting state with blurred grain boundary and silicic content on the slipping surface (Table 3). Meanwhile, the craze structure is also distinguished from the special polygonal shape and morphology (Fig. 6).

In previous studies, mechanical scientists verified that relative fracture phenomena in the craze structures, such as void, hole, pore, crack, fissure, and damage of boundary plane, result from discontinuous changes between stress field-displacement field-temperature field in the deformed process (Yang, 1996), which reflect a ductile/brittle transition or strengthening mechanism (Luo and Yang, 2003).

In conformance to analyses of textural phenomena and mechanical characters, the five structures of nanoscale pore and crack could be sorted out into three types, i.e., contraction (containing relaxation), delamination (containing exfoliation) and craze.

Table 3. Calculated data of the energy spectrum analysis.

Item		Molecular formula (%)						
		SiO_2	Al_2O_3	Fe_2O_3	MgO	CaO	K_2O	CO_2
Outer layer	Molecular content	51.21	3.91	0.40	2.12	-	-	41.88
	Weight	55.81	7.23	1.15	1.55	-	-	33.43
	Molecular content	37.66	8.17	1.59	3.70	1.10	1.11	46.67
	Weight	39.57	14.56	4.44	2.61	1.07	1.07	35.92
Inner layer	Molecular content	35.00	8.62	1.21	4.42	1.01	1.20	48.54
	Weight	37.16	15.53	3.43	3.14	1.00	2.00	37.74
	Molecular content	34.23	8.10	1.17	3.66	0.83	1.14	50.83
	Weight	36.66	14.72	3.33	2.63	0.83	1.91	39.91

Table 4. Main parameters of inclusions in sub-well layers of Paleozoic Erathem in the North Shaanxi region (Guo et al., 2002).

No.	Depth (m)	Homogeneous temperature (°C)	Homogeneous pressure (MPa)	Relative salinity	Density (g/cm^3)	Collation temperature (°C)	Catching temperature (°C)	Catching pressure (MPa)
53	3648	145	7.122	17.52	1.048248	16	161	21.475
53	3648	162	22.399	17.34	1.032964	36	198	57.799
53	3648	164	23.357	17.43	1.032007	36	200	59.866
156	3266.32	190	20.485	13.72	0.979288	30	220	49.349
156	3266.32	197	26.901	14.36	0.977697	35	232	61.498
156	3266.32	219	48.330	14.36	0.955827	56	275	111.532

4. Shale gas reservoir effect

The shale gas reservoir effect involves two kinds of adsorptive power and storage action for the shale gas (adsorbed state and free state).

4.1 Adsorption-gas effect

A variation of micro-nano pores and cracks mentioned above all occur in the shear thin layer, and they are constructed by the nanograin-nano line-nano layer (Figs. 1, 2, 4 and 5). Obviously, a nanograin itself must lead to multiple functions, such as the nanoscale effect, nano-surface effect and nano-interface effect (Veprek et al., 2000). At the macroscopic scale, geologists regard kerogen and clay-particle surfaces as principal sites of adsorbed gas (Curtis, 2002). Obviously, the dominant role of nanoparticles in gas adsorption should be determined. This is due to the following reasons: (1) The larger surface area of the nanograins; (2) The larger thickness of the nano-grain layer (lamellae, foliation and schistose structures). On the one hand, the shear slip thin layer intrinsically demonstrates superposed lamellae development in the shale; on the other hand, nanominerals like sericite and penninite, which belong to the products of dynamic metamorphism under lower temperature (APraiz and Eguiluz, 2002) (150-200 °C, Table 4), distribute in shear slip thin layers layer by layer. Most significantly, the larger thickness contained in the nanograin layer has undergone three developing stages and produced the different structures of nanoscale pore and crack motioned above.

4.2 Storage-gas effect

During the past ten years, matrix-related pores from nanometer to micrometer size in the shales have been subdivided into three types, i.e., inter-particle pore (inter P), intra-particle pore (intra P), and organic matter pore (Curtis, 2002). These fracture pores are not controlled by the individual matrix particle. Besides, the morphology of the pores could possess largely jagged, high-aspect, and crescent-shaped features (Desbois et al., 2009). Thus, these pores are considered to be similar to the “pore and crack” cited above in many ways. As compared with the matrix-related pores, nanoscaled pore and crack formed by the shear slip action have conspicuous features for the storage-gas effect:

1) Slipping grooves on the shear slip plane often occur in various nanoscale pore and crack structures (Figs. 7(a) and 7(b)), especially in the contraction structure type (including the relaxation type), and the latter could extend along the groove bottom with a better storage-gas space.
2) At the nanometer to micrometer level, crack development is closely associated with the pore, forming the pore and crack unit, and this phenomenon is highly prominent in

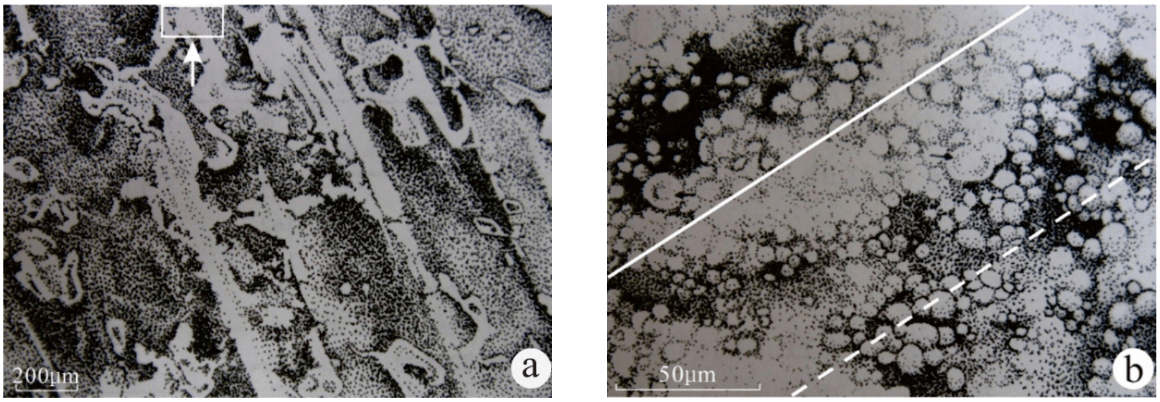

Fig. 7. SEM images of slipping grooves and ridges (Sun et al., 2005): (a) Slipping lines have ridge-like risen structures, and slipping grooves parallel to the ridges (bright domains) emerge out of the contraction pores and cracks (black domains). The arrow shows a microdomain after magnified observation (Fig. 7(b)); (b) The concentrated grains form raised ridges (direction of solid line), and the sparse grains take shape depressions (direction of dashed line), in which contraction pores occur at the bottom of the groove along the orienting stretch (black domains).

the craze structure (Fig. 6). Meanwhile, the evolution of varied pore and crack in terms of spatial and temporal distribution may constitute a network texture (Berger, 1990; Gao et al., 2020) caused by compound and superimposition, which could act as a given controlling factor in the storage and permeability of free gas.

3) Matrix-related pores commonly have crack-like tips, a preferred orientation parallel to bedding (Desbois et al., 2009). Therefore, to recognize their genetic mechanism, the nano-confinement layer and strain weakening slipping need to be investigated (Musil, 2000; Holdsworth, 2004). Thus, both the matrix-related pores and the delamination structure could have an intimate connection with respect to one another. This being the case, the structure of the nanoscale pore and crack might be well-recognized for the storage-gas effect from one aspect.

5. Conclusions

1) Layered slipping easily occurs in the shale, and the shear thin layers, which consist of nanograins and nanominerals, widely and regionally distribute on shear slip planes under the nanocoating action. Those shear nanograin layers are a reiterative superimposition following the regional layer slipping tectonism.
2) The developing process of the nanocoating texture of the shear slip planes can be subdivided into three stages: viscoelastic deformation stage, rheological deformation stage and embrittling deformation stage, which can produce three types of nanoscale pore and crack structure: contraction, relaxation and exfoliation. Two other structures are also found in the shales, namely the delamination structure and the craze structure.
3) The nanoparticle itself is responsible for a larger nanosurface effect and adsorption gas effect, and three types of pore and crack structure could play a given controlling factor in free gas storage and permeability. The single layer of the nanograin coating is much thinner, but the whole thickness and distribution form a regional trend. The matrix-related pores and the delamination pore and crack are intimate connections for the forming mechanisms and origin. Overall, the establishment of the three types of pore and crack structure is a worthy supplement to shale matrix-related pore classification.

Acknowledgement

This research was financially supported by the National Natural Science Foundation of China (Nos. 41872160, 41530315), the Fundamental Research Funds for the Central Universities. We thank Profs. Dezi Wang and Youwei Du from Nanjing University and Prof. Wanlin Guo from Nanjing University of Aeronautics & Astronautics for their valuable suggestions. We also thank Prof. Xueyi Wu from the Institute of Geochemistry, Chinese Academy Sciences, Senior Engineer Chunchao Wang from the Institute of Geology and Paleontology, Chinese Academy Sciences and Mr. Honglong Chen from Gong Yuanlu Middle School, Nanjing, for their assistance in the HT/HP experiment, SEM observation and physical-mechanical parameter determination.

Conflict of interest

The authors declare no competing interest.

References

Apraiz, A., Eguiluz, L. Hercynian tectono-thermal evolution associated with crustal extension and exhumation of the Lora del Rio metamorphic core complex (Ossa-Morena zone, Iberian Massif, SW Spain). International Journal of Earth Sciences, 2002, 91(1): 76-92.

Aringhieri, R. Nanoporosity characteristics of some natural clay minerals and soils. Clays and Clay Minerals, 2004,

52(6): 700-704.

Berger, L. L. On the mechanism of craze fibril breakdown in glassy polymers. Macromolecules, 1990, 23(11): 2926-2934.

Braun, O. M., Naumovets, A. G. Nanotribology: Microscopic mechanisms of friction. Surface Science Reports, 2006, 60(6-7): 79-158.

Chen, G., Dong, D., Wang, S., et al. A preliminary study on accumulation mechanism and enrichment pattern of shale gas. Natural Gas Industry, 2009, 29(5): 17-21, 134-135. (in Chinese)

Chen, L., Jiang, Z., Liu, K., et al. Quantitative evaluation of free gas and adsorbed gas content of Wufeng-Longmaxi shales in the Jiaoshiba area, Sichuan Basin, China. Advanced in Geo-Energy Research, 2017, 1(2): 112-123.

Comer, J. B. Reservoir characteristics and production potential of the Woodford shale. World Oil, 2008, 229(8): 83-87.

Curtis, J. B. Fractured shale gas systems. AAPG Bulletin, 2002, 86(11): 1921-1938.

De Paola, N. Nano-powder coating can make fault surfaces smooth and shiny: Implications for fault mechanics? Geology, 2013, 41(6): 719-720.

Desbois, G., Urai, J. L., Kukla, P. A. Morphology of the pore space in claystones-evidence from BIB/FIB ion beam sectioning and cryo-SEM observations. eEarth Discusion, 2009, 4(1): 1-19.

Gale, J. F. W., Reed, R. M., Holder, J. Natural fractures in the Barnett shale and their importance for hydraulic fracture treatments. AAPG Bulletin, 2007, 91(4): 603-622.

Gao, Z., Fan, Y., Xuan, Q., et al. A review of shale pore structure evolution characteristics with increasing thermal maturities. Advanced in Geo-Energy Research, 2020, 4(3): 247-259.

Goodwin, L. B., Wenk, H. R. Development of phyllonite from granodiorite: Mechanisms of grain-size reduction in the Santa-Rosa mylonite zone, California. Journal of Structural Geology, 1995, 17(5): 689-697, 699-707.

Guo, J., Sun, Y., Zhu, W., et al. A new explanation for the genetic mechanism on the smear efficiency within oil-gas sealing covers. Journal of Nanjing University (Natural Sciences), 2002, 38(6): 766-770. (in Chinese)

Guo, W., Dong, H., Lu, M., et al. The coupled effects of thickness and delamination on cracking resistance of X70 pipeline steel. International Journal of Pressure Vessels and Piping, 2002, 79(6): 403-412.

Hirose, T., Bystricky, M., Kunze, K., et al. Semi-brittle flow during dehydration of lizardite-chrysotile serpentinite deformed in torsion: Implications for the rheology of oceanic lithosphere. Earth and Planetary Science Letters, 2006, 249(3-4): 484-493.

Hochella, M. F., Lower, S. K., Maurice, P. A., et al. Nanominerals, mineral nanoparticles and earth systems. Science, 2008, 319(5870): 1631-1635.

Holdsworth, R. E. Weak faults-Rotten cores. Science, 2004, 303(5655): 181-182.

Hunt, G. W., Peletier, M. A., Wadee, M. A. The maxwell stability criterion in pseudo-energy models of kink banding. Journal of Structural Geology, 2000, 22(5): 669-681.

Janssen, C., Wirth, R., Reinicke, A., et al. Nanoscale porosity in SAFOD core samples (San Andreas Fault). Earth and Planetary Science Letters, 2011, 301(1-2): 179-189.

Javadpour, F. Nanopores and apparent permeability of gas flow in mudrocks (shales and siltstone). Journal of Canadian Petroleum Technology, 2009, 48(8): 16-21.

John, W., Roger, R. The shale shaker: An investor's guide to shale gas. Oil and Gas Investor, 2007, 1: 2-9.

Ju, Y., Huang, C., Sun, Y., et al. Nanogeosciences: Research history, current status, and development trends. Journal of Nanoscience and Nanotechnology, 2017, 17(9): 5930-5965.

Ju, Y., Huang, C., Sun, Y., et al. Nanogeology in China: A review. China Geology, 2018, 1: 286-303.

Ju, Y., Yu, Q., Fang, L., et al. Chinese shale gas reservoir types and their controlling factors. Advances in Earth Science, 2016, 31(8): 782-799. (in Chinese)

Kambe, N. Highly-uniform nano-structured building blocks of metal-(O, C, N, S) and their complex compounds. Scripta Materialia, 2001, 44(8-9): 1671-1675.

Keulen, N., Heilbronner, R., Stuenitz, H., et al. Grain size distributions of fault rocks: A comparison between experimentally and naturally deformed granitoids. Journal of Structural Geology, 2007, 29(8): 1282-1300.

Krása, D., Wilkinson, C. D. W., Gadegaard, N., et al. Nanofabrication of two-dimensional arrays of magnetite particles for fundamental rock magnetic studies. Journal of Geophysical Research: Solid Earth, 2009, 114: B02104.

Li, K. J., Kong, S. Q., Xia, P., et al. Microstructural characterisation of organic matter pores in coal-measure shale. Advances in Geo-Energy Research, 2020, 4(4): 372-391.

Lin, A. M. Fossil Earthquakes: The Formation And Preservation of Pseudotachylytes. New York, USA, Springer, 2008.

Long, P., Zhang, J., Tang, X., et al. Feature of muddy shale fissure and its effect for shale gas exploration and development. Natural Gas Geoscience, 2011, 22(3): 525-532. (in Chinese)

Loucks, R. G., Reed, R. M., Ruppel, S. C., et al. Morphology, genesis, and distribution of nanometer-scale pores in siliceous mudstones of the Mississippian Barnett shale. Journal of Sedimentary Research, 2009, 79(11-12): 848-861.

Loucks, R. G., Reed, R. M., Ruppel, S. C., et al. Spectrum of pore types and networks in mudrocks and a descriptive classification for matrix-related mudrock pores. AAPG Bulletin, 2012, 96(6): 1071-1098.

Lu, X., Sun, Y., Shu, L., et al. Cataclastic rheology of carbonate rocks. Science in China Series D: Earth Sciences, 2005, 48(8): 1227-1233.

Luo, W., Yang, T. Crack tip damage and crazing in polymers under loading. Acta Mechanica Sinica, 1990, 35(5): 553-560. (in Chinese)

Luo, W., Yang, T. Computer simulation of conic-shaped patterns on fracture surfaces of polymers. Journal of Applied Polymer Science, 2003, 89(6): 1722-1725.

Masch, L., Wenk, H. R., Preuss, E. Electron microscopy study of hyalomylonites-evidence for frictional melting

in landslides. Tectonophysics, 1985, 115(1-2): 131-160.

Mclaren, A. C., Pryer, L. L. Microstructural investigation of the interaction and interdependence of cataclastic and plastic mechanisms in feldspar crystals deformed in the semi-brittle field. Tectonophysics, 2001, 335(1-2): 1-15.

Montgomery, S. L., Jarvie, D. M., Bowker, K. A., et al. Mississippian Barnett shale, Fort Worth basin, north-central Texas: Gas-shale play with multi-trillion cubic foot potential. AAPG Bulletin, 2005, 89(2): 155-175.

Morley, C. K., von Hagke, C., Hansberry, R. L., et al. Review of major shale-dominated detachment and thrust characteristics in the diagenetic zone: Part I, meso- and macro-scopic scale. Earth-Science Reviews, 2017, 173: 168-228.

Musil, J. Hard and superhard nanocomposite coatings. Surface and Coatings Technology, 2000, 125(1-3): 322-330.

Raimbourg, H., Toyoshima, T., Harima, Y., et al. Grain-size reduction mechanisms and rheological consequences in high-temperature gabbro mylonites of Hidaka, Japan. Earth and Planetary Science Letters, 2008, 267(3-4): 637-653.

Slatt, R. M., O'Brien, N. R. Pore types in the Barnett and Woodford gas shales: Contribution to understanding gas storage and migration pathways in fine-grained rocks. AAPG Bulletin, 2011, 95(12): 2017-2030.

Sun, Y., Ge, H., Lu, X., et al. Discovery and analysis of the ultra-micro nano texture in the ductile-brittle shear zone. Science China Earth Sciences, 2003, 33(7): 619-625. (in Chinese)

Sun, Y., Jiang, S., Zhou, W., et al. Mechanical analysis and identification markings of nanoparticle distribution in narrow friction zones. Advanced Materials Research, 2014a, 924: 312-318.

Sun, Y., Jiang, S., Zhou, W., et al. Nano-coating texture on the shear slip surface in rocky materials. Advanced Materials Research, 2013, 669: 108-114.

Sun, Y., Ju, Y., Jiang, S., et al. A preliminary identification of micro/nano scale textures on mineralization, hydrocarbon accumulation and seismic formation structure. Journal of Nanoscience and Nanotechnology, 2017, 17(9): 7048-7054.

Sun, Y., Ju, Y., Wang, G., et al. Five types of micro/nano pore-crack in shale and their unconventional gas accumulation effect. Paper Presented at 2014 Annual Meeting of Chinese Geoscience Union-Topic 57: Basin Dynamics and Unconventional Energy, Peking, 20 October, 2014b. (in Chinese)

Sun, Y., Lu, X., Ju, Y. Nano texture and mineralization in fault shear zones. Geological Journal of China Universities, 2018, 24(3): 307-324. (in Chinese)

Sun, Y., Lu, X., Liu, D., et al. Discovery, nomenclature of the centimeter scale grinding gravels and the nanometer scale grinding grains in fault shearing zones and the significance for oil-gas geology. Geological Journal of China Universities, 2005, 11(4): 521-526. (in Chinese)

Sun, Y., Lu, X., Zhang, X., et al. Nano-texture of penetrative foliation in metamorphic rocks. Science in China Series D: Earth Sciences, 2008a, 51(12): 1750-1758.

Sun, Y., Shu, L., Lu, X., et al. A comparative study of natural and experimental nano-sized grinding grain textures in rocks. Chinese Science Bulletin, 2008b, 53(8): 1217-1221.

Sun, Y., Shu, L., Lu, X., et al. Recent progress in studies on the nano-sized particle layer in rock shear planes. Progress in Natural Science, 2008c, 18(4): 367-373.

Suvorov, A. I. Tectonic layering and tectonic motions in the continental lithosphere. Geotectonics, 2000, 34(6): 442-451.

Tahirkheli, S. N. COMMENT-Becoming Digital-As we call for information that is born digital, what will happen to the legacy of information that must become digital? Geotimes, 2001, 46(1): 5-5.

Urbakh, M., Klafter, J., Gourdon, D., et al. The nonlinear nature of friction. Nature, 2004, 430(6999): 525-528.

Veprek, S., Niederhofer, A., Moto, K., et al. Composition, nanostructure and origin of the ultrahardness in nc-TiN/a-Si_3N_4/a- and nc-$TiSi_2$ nanocomposites with H_v=80 to $\geq$105 GPa. Surface and Coatings Technology, 2000, 133-134: 152-159.

Wang, C., Sun, Y. Oriented microfractures in Cajon pass drill cores: Stress field near the San Andreas fault. Journal of Geophysical Research: Solid Earth and Planets, 1990, 95(B7): 11135-11142.

Wang, G., Ju, Y. Organic shale micropore and mesopore structure characterization by ultra-low pressure N_2 physisorption: Experimental procedure and interpretation model. Journal of Natural Gas Science and Engineering, 2015, 27: 452-465.

Wang, Y., Gao, H., Xu, H. Nanogeochemistry: Nanostructures and their reactivity in natural systems, in Frontiers in Geochemistry: Contribution of Geochemistry to the Study of the Earth, edited by R. Hamon and A. Parker, Blackwell, New Jersey, pp. 200-220, 2011.

Yang, T. Rheology of bodies with defects. Mechanics and Practice, 1996, 18(3): 13-17. (in Chinese)

Zhu, H., Ju, Y., Huang, C., et al. Pore structure variations across structural deformation of Silurian Longmaxi Shale: An example from the Chuandong Thrust-Fold Belt. Fuel, 2019, 241: 914-932.